The Astrophysical Journal, 652:1122–1128, 2006 December 1

HIDDEN TRIGGER FOR THE GIANT STARBURST ARC IN M83?

Rubén J. Díaz,[1,2] Horacio Dottori,[3] Maria P. Aguero,[2] Evencio Mediavilla,[4]
Irapuan Rodrigues,[3] and Damian Mast[2]
Received 2006 June 9; accepted 2006 July 17

ABSTRACT

The huge star formation events that occur at some galactic centers do not provide enough clues as to their origin, since the morphological signatures of the triggering mechanism are smeared out in the timescale of a few orbital revolutions of the galaxy core. Our high spatial resolution three-dimensional near-infrared spectroscopy for the first time reveals that a previously known hidden mass concentration is located exactly at the youngest end of a giant star-forming arc. This location, the inferred average cluster ages, and the dynamical times clearly indicate that the interloper has left behind a spur of violent star formation in M83, in a transient event lasting less than one orbital revolution. The study of the origin (bar funneling or cannibalized satellite) and fate (black hole merging or giant stellar cluster) of this system could provide clues to the question of core growing and morphological evolution in grand-design spiral galaxies. In particular, our TreeSPH numerical modeling suggests that the two nuclei could coalesce, forming a single massive core in about 60 million years or less. This work is based on observations made at the Gemini South Telescope.

Subject headings: galaxies: active — galaxies: individual (M83) — galaxies: ISM — galaxies: kinematics and dynamics — galaxies: nuclei — galaxies: starburst

1. INTRODUCTION

The enormous energy output detected in many cores of galaxies is one of the key issues in the study of galaxies and their evolution; notwithstanding, several questions remain unsolved. Are accretion onto supermassive black holes and violent star formation just co-evolving phenomena or necessary partners of the activity? How is the detailed physics of the mechanisms triggering the nuclear extended violent star formation? What is the relationship of the triggering mechanisms to galaxy evolution? The main challenge facing these issues is that developed stages of large star formation events at galactic centers do not provide sufficient clues to their origin, since the morphological signatures of the triggering mechanism are smeared out on the timescale of a few orbital revolutions of the galaxy core. Here we present the discovery of hidden evolutionary links in one of the extraordinary transient events in the life of a galaxy like our own, which occur when the remnant of an accreted (galactic or extragalactic) body arrives at the galactic nuclear region. For M83, this arrival is accompanied by the fireworks of the violent star formation arising in the gas-rich environment of this galaxy, giving us the unique opportunity in the nearby universe for studying the detailed physics of the so-called nuclear starbursts and the initial stages of the supermassive black hole growth in the center of galaxies.

M83 is a galaxy with grand-design spiral structure and could be taken at first glance to be one of the nearest (distance 3.7 Mpc; RC3) normal spiral galaxies. Its central region has progressively gained attention since it was known to harbor the nearest "hot spot" or Sersic-Pastoriza nucleus (Sersic & Pastoriza 1965), later identified as one of the brightest nearby giant H II complexes (Arsenault & Roy 1986), and now studied as the nearest nuclear massive starburst (Fig. 1). It has been subject of several detailed observational studies, including a wealth of observations with the Very Large Telescope (VLT) and the *Hubble Space Telescope* (*HST*), but the dynamical origin of the starburst has remained elusive. Several hypotheses have been discussed, from the influence of a not very close companion (Rogstad et al. 1974) or the resonance patterns of the global weak bar (Elmegreen et al. 1998; Petitpas & Wilson 1998), down in scale to the presence of a nuclear bar in the morphology at near- and mid-infrared spectral ranges (Gallais et al. 1991). Clues to the dynamical signature of a trigger have been provided initially by long-slit observations of the nuclear region in a study by Thatte et al. (2000), who report two peaks in the slit profile of the stellar radial velocity dispersion. The lack of spatially extended spectroscopic information did not allow them to fix the position and to confirm the presence of a second nucleus. This result was interpreted as revealing the presence of two dynamical centers, possibly the consequence of the off-center nuclear bar postulated in previous low-resolution studies (Gallais et al. 1991; Telesco 1988). However, the existence of an off-centered nuclear bar is not expected from observations and modeling (Maciejewski & Sparke 2000; Heller & Shlosman 1994). The existence of two off-centered nuclei, one of them coincident with the optical nucleus and the other located a few arcseconds to the west of the optical nucleus, was proposed (Mast et al. 2002, 2006) by a team using the Multifunctional Spectrograph at the Bosque Alegre Astrophysical Station (Díaz et al. 1999) to determine the ionized gas radial velocity and radial velocity dispersion fields from the optical emission.

A deep study (Harris et al. 2001) of the violent star formation taking place in M83 was made by a thorough photometric analysis of the 45 most massive clusters in the giant star-forming arc of M83 with the Wide Field Planetary Camera 2 of the *HST*. This giant arc is located between 3″ and 7″ from the galaxy center, spans about 15″ (255 pc), and includes about 20 massive young clusters similar to 30 Dor, one of the largest young clusters in the Local Group of galaxies. By comparing the broad- and

[1] Gemini Observatory, Southern Operations Center, Chile; rdiaz@gemini.edu.
[2] Observatorio Astronómico de Córdoba, Universidad Nacional de Córdoba and CONICET, Argentina.
[3] Instituto de Física-Universidade Federal do Rio Grande do Sul, Brazil.
[4] Instituto de Astrofisica de Canarias, Spain.

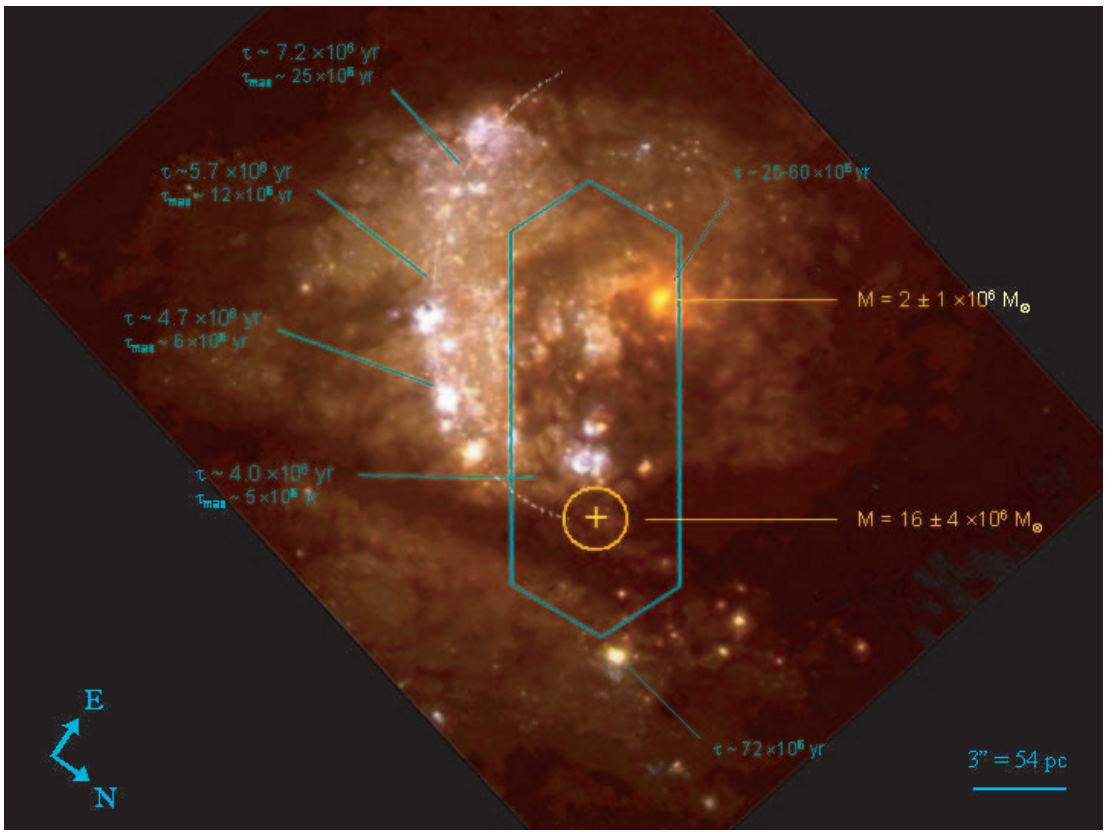

FIG. 1.— *HST* false color optical image, combined from F439W, F555W, and F702W filters. Point-spread functions were matched to a common resolution of 0.″09. We determined the average ages of the young massive star clusters in the arc (in 25° angular sectors) by using the available data (Harris et al. 2001), which are depicted together with the age of the oldest clusters in each sector. The integral field observed with the CIRPASS instrument attached to the Gemini South telescope has been depicted together with the position of the main rotation center found (the yellow circle corresponds to the 2 σ uncertainty radius). The red features in the image inside the integral field area can be compared with the *J*-band continuum image generated from the spectral data in Fig. 2. Note that the rotation center (intruder nucleus) is at the youngest end of the partial ellipse that describes the positions of the main star-forming regions in the giant arc. Coincidentally, the dynamical crossing time at this scale is about 5 Myr. This evidence is consistent with a trail of violent star formation triggered by the passage of the intruder nucleus.

narrowband photometry with theoretical population synthesis models, the age and mass of each cluster were estimated (Harris et al. 2001). The main conclusion was that the starburst began $\lesssim$10 Myr ago and that the clusters may dissolve on a 10 Myr timescale. More recently, Sakamoto et al. (2004) studied the CO emission in M83 with the Submillimeter Array and found that the distribution and kinematics of the molecular gas is typical for barred galaxies down to 1 kpc radii, although they confirm unusual kinematics around the double nucleus in the central $\sim$300 pc. The relatively low spatial resolution of the velocity field ($\sim$3″) leads these authors to conclude that the second nucleus would coincide with the center of the bulge. They discuss the dynamics of the M83 central region in the context of the bar instability and inner Lindblad resonance of the disk and conclude that the nuclear starburst of M83 owes much to the bar-driven gas dynamics for accumulating molecular gas toward the central 300 pc.

In order to understand the nature of the double nucleus configuration and its possible relation to the giant arc of star formation, minimizing the effects of dust and improving the relative low spatial resolution ($\sim$2″) of our previous optical observations, we applied the new observational techniques of three-dimensional (3D) spectroscopy at near-infrared (NIR) wavelengths performed at subarcsecond spatial resolution. We complement these new observations with numerical simulations, which reveal what can be considered a growing galactic core in a grand-design spiral galaxy.

2. OBSERVATIONS

2.1. *Observations*

We used the Cambridge Infrared Panoramic Survey Spectrograph (Parry et al. 2000), built at the Cambridge Institute of Astronomy, during its visit to the Gemini South 8.1 m telescope in March 2003. The observations were taken with an Integral Field Unit (IFU) sampling of 0.″36 (6.4 pc) in an elliptical arrangement with a size of 13″ × 5″. The array has 490 hexagonal doublet lenses attached to fibers and provides an area filling factor near 100%. The IFU was oriented at PA 120° (Fig. 1) and was centered in a point midway between the optical nucleus position and the possible position of the hidden nucleus previously determined from our optical 2D kinematics (Mast et al. 2002). The set of 490 spectra covers the spectral range 1.2–1.4 μm, including the emission lines Paβ 1.3 μm and [Fe II] 1.26 μm, and the spectral resolution is $\sim$3200. During the observations the peripheral wave front sensor of Gemini active optics was used, and the achieved image quality was excellent (FWHM $\approx$ 0.″5); therefore, the focal plane was somewhat subsampled by the used configuration. The data were reduced using IRAF (distributed by the National Optical Astronomy Observatory), ADHOC (2D kinematics analysis software developed by Marseille's Observatory), SAO (spectra processing software developed by the Special Astrophysical Observatory, Russia), and standard worksheets and image processing software. Due to the complex data output, the spectra have been

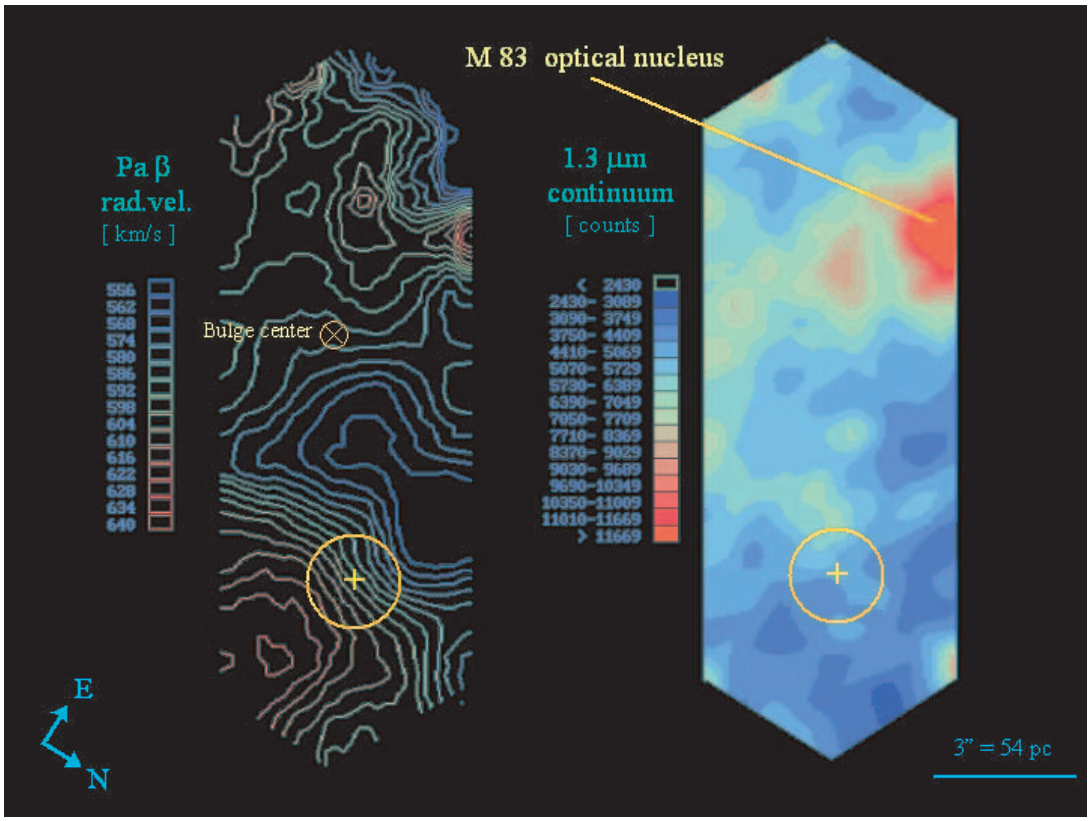

FIG. 2.—*Left:* Radial velocity map of the ionized gas, corresponding to the main integral field observed with both nuclei. It corresponds to the field marked in Fig. 1. The step in isovelocity lines is set equal to the average uncertainty, but the shape of the field does not qualitatively change even at a 3 σ display. *Right:* Image generated from the continuum emission in the spectral region 1.28 μm (in the photometric *J*-band domain); the achieved resolution is 0.″6. The main features can be compared for reference with the reddest features in Fig. 1. The yellow circle corresponds to the 2 σ uncertainty radius, and it is evident that the main rotation center is dark at *J*-band wavelengths and is located far from the visible nucleus position and from the geometrical center of the galactic bulge at near-infrared wavelengths, which is marked with a cross.

carefully reduced one by one, using the prominent sky emission lines as wavelength and profile references. The general techniques used have been previously described in other works (Díaz et al. 1999; Mast et al. 2006). In most of the field the S/N ratio was higher than 10, and the average radial velocity uncertainty resulted about 6 km s^{-1}. We present here a mean velocity field that includes both nuclei. We also constructed the Paβ continuum map, which is shown in Figure 2 and can be compared for reference with the *HST* pseudocolor optical image, combined from F439W, F555W, and F702W filters, presented in Figure 1.

2.2. *Astrometry*

The position reference system was taken from the two most recent papers that show optical and NIR images with accurate astrometry (Thatte et al. 2000; Harris et al. 2001), which have coordinate system differences of about 0.″1 (determined from their figures). Using some *J*-band compact features appearing in Figure 2 as position references and identifying them in the previous high-resolution images (mainly the one at F814W band), we were able to provide coordinates for the galaxy visible nucleus (defined as the continuum emission peak), the bulge geometrical center, and the dark rotation center reported here. The resulting coordinates of the visible nucleus are $\alpha = 13^h37^m0^s.95$, $\delta = -29°51'55''.5$ (J2000.0) with a 2 σ uncertainty of 0.″15. The bulge geometrical center, defined as the symmetry center of the outer *K*-band isophotes of the galactic central region (Thatte et al. 2000; central arcminute, $r < 500$ kpc), is at $\alpha = 13^h37^m0^s.57$, $\delta = -29°51'56''.9$ (J2000.0), with a 2 σ uncertainty of 0.″8 arising mainly in the photometric determination of this symmetry center. Finally, the position of the dark rotation pattern center was determined by fitting a pure rotational model (Satoh disk; Binney & Tremaine 1991, pp. 44–45) with varying inclination. The resulting coordinates are $\alpha = 13^h37^m0^s.46$, $\delta = -29°51'53''.6$ (J2000.0), with a 2 σ uncertainty of 0.″7.

3. RESULTS AND DISCUSSION

We present in Figure 2 the radial velocity field of the ionized gas observed at NIR wavelengths. An inspection of the continuum map (with a resolution of 0.″6) and the radial velocity field clearly shows that the main rotation center is far (7.″8 $\pm$ 0.7″ or 140 $\pm$ 13 pc to the WNW, P.A. = 284° $\pm$ 5°) from the optical nucleus position, defined as the maximum peak in the *J*-band continuum emission. The optical nucleus is also located out of the global symmetry center: the galactic bulge or central spheroid geometry center is located at 3.″5 $\pm$ 0.″8 or 63 $\pm$ 14 pc to the WNW, P.A. = 249° $\pm$ 5°, from the visible nucleus position. The relative positions of the visible nucleus, the bulge geometrical center, and dark rotation center can be seen in Figures 2 and 3. The radial velocity gradient across the optical nucleus implies a total mass not larger than $10^7 M_\odot$ inside a radius of 2″. In particular, the fit of a Satoh disk model yields a total mass of $(2 \pm 1) \times 10^6 M_\odot$ with an inclination of 50° $\pm$ 10°. This dynamical mass value is consistent with the mass calculated (Thatte et al. 2000) for the stellar component, using population synthesis models. The main rotation center has no obvious emitting structure associated in the continuum map of Figure 2 and in the NIR *HST* imagery, but is coincident with the largest lobe in the 10 μm map (Gallais et al. 1991) shown in Figure 3, and the

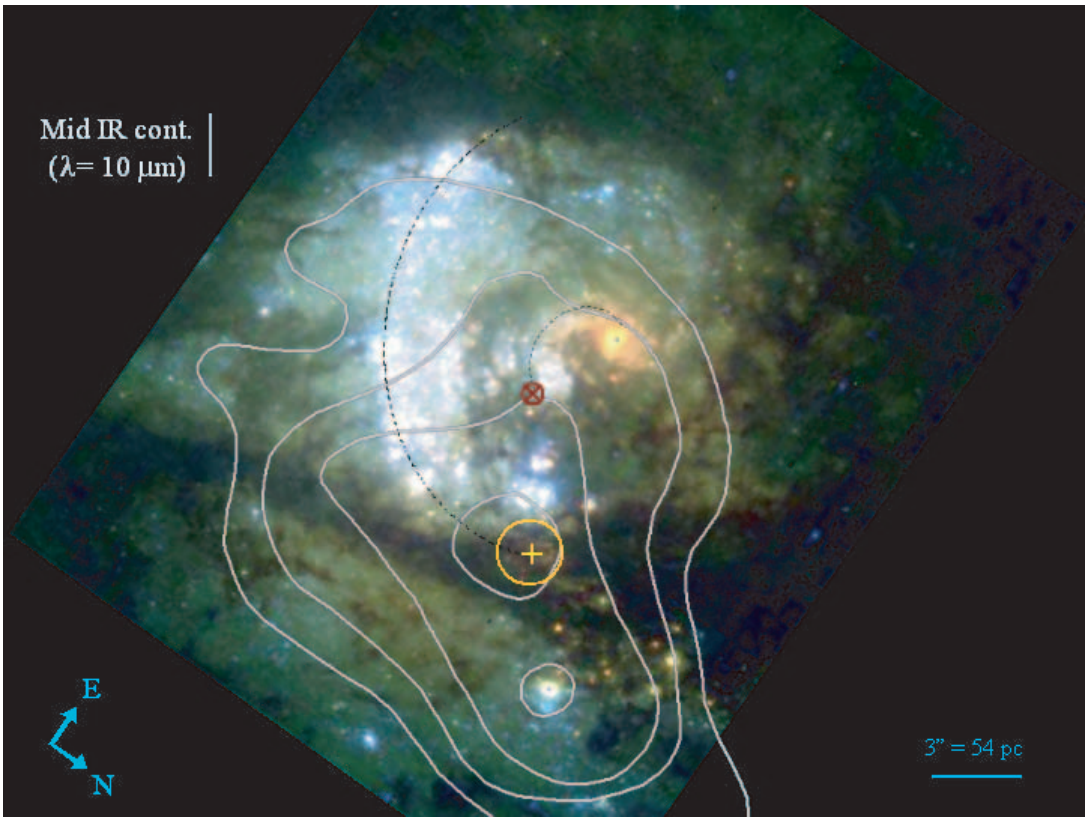

FIG. 3.—Image constructed from the filters F300W, F547M, and F814W. In this display the youngest clusters of the field are enhanced. A strong tidal shape can be seen in the mid-infrared continuum map at 10 μm wavelengths (Telesco 1988), which is depicted in gray isophotes using the corresponding position references (Gallais et al. 1991). The position uncertainty of the rotation center corresponding to the intruder nucleus is marked with a circle. Strikingly, this position is also coincident with the largest lobe in the mid-infrared emission. Note the partial ellipses that describe the main regions in the giant arc and a possible stellar trail of the optical nucleus.

second largest lobe in the 6 cm radio map (Telesco 1988). The rotation pattern has been fitted with a Satoh disk (Binney & Tremaine 1991) with inclination $50^\circ \pm 15^\circ$ and a total mass of $(16 \pm 4) \times 10^6\ M_\odot$. Considering the lack of emission in our 1.3 μm continuum map of this highly obscured region, we estimate that it should have a mass-to-light ratio 10–100 times larger than the optical nucleus in the J band. The relatively large mass of the intruder would explain the optical nucleus off centering and perturbed appearance in the high-resolution images. The maximum possible central mass of this dark rotation center can be estimated by fitting a pointlike gravitational source to the observed radial velocity gradient, inside a $1''$ radius from the rotation center and considering a beam smearing of two sampling elements ($0''.72$). Therefore, the largest supermassive black hole that can be fitted to the unresolved inner region of the rotation center should have a mass not larger than $(3 \pm 1) \times 10^6 (\sin i)^{-1}\ M_\odot$.

The hidden mass concentration is located precisely at the younger end of the star forming arc, in a region where star clusters with extinction possibly larger than 10 mag have been reported (Gallais et al. 1991; Mast et al. 2006). Therefore, the core of the hidden mass concentration could eventually be explained by the presence of one or a few supermassive star clusters such as the one forming the optical nucleus (stellar luminosity corresponding to $2.5 \times 10^6\ M_\odot$; Thatte et al. 2000), but highly obscured in this case.

This obscured rotation center (hereafter intruder nucleus) could correspond to an interloper gaseous body funneled to the circumnuclear environment by the global bar dynamics in a scenario such as that proposed by Elmegreen et al. (1998) for M83. This kind of scenario has been thoroughly modeled by several teams (e.g., Heller & Shlosman 1994; Pinner et al. 1995), but until now there was no direct observational evidence of the behavior of the central region during a bar-fueling event, so the results presented here could be important for testing the detailed physics of the models. Currently the best and unbiased (in terms of extinction) picture of the bar dynamics in M83 is the interferometric imaging of CO emission (Sakamoto et al. 2004). Based on a relatively low spatial resolution velocity field, these authors conclude that the second nucleus would coincide with the center of the bulge and that the optical nucleus could be an interloper. The dynamics of the M83 bar instability and resonances have been extensively discussed by Sakamoto et al. (2004) and by other authors previously (e.g., Handa et al. 1990; Kenney & Lord 1991; Elmegreen et al. 1998), and the main conclusion that can be drawn is that, whatever the trigger, the nuclear starburst of M83 owes much to the bar for the accumulation of molecular gas in the central region. Although the Sakamoto et al. (2004) velocity map has much lower (5–8 times) resolution than the Gemini+CIRPASS data discussed here, a slight distortion and isovelocities crowding along the minor axis and northwest from the optical nucleus position could be identified as the hidden mass concentration. This concentration is located just at the edge of a fairly massive molecular gas concentration in what could be interpreted as bar streaming flow of M83, but it appears strongly asymmetric in intensity and shape with respect to the global pattern.

It could be possible that the hidden nucleus is part of the material fed by the bar, but this would imply that the bar is capable of funneling extended bodies of 10 million solar masses and tens

of parsec sizes to the circumnuclear region. Moreover, the bar feeding scenario is difficult to support due to a couple of details:

1. The strong asymmetrical appearance of the mid-infrared (Fig. 3) and radio maps (λ6 cm; Telesco 1988), which, in addition to their tidal shape, would not show a continuity of their features with the bar dust lanes (marking the main bar streaming regions; Athanassoula 1992).
2. There is at least one other case of a single nucleus off center with respect to both the geometric and the kinematical center, in the strongly barred Seyfert galaxy NGC 1672 (Díaz et al. 1999). In both NGC 1672 and M83 the strong offset between the optical nucleus, the bulge center, and the main kinematic center would indeed remain as a puzzle in a bar-funneling scenario. Nevertheless, this scenario cannot be ruled out without high-resolution numerical models.

An alternative would be the arrival of an accreted satellite core into the highly gaseous circumnuclear environment of M83. As this is a theoretical scenario less explored at the scale of our observations, we will thoroughly analyze the possibilities in the present case of M83.

Malin & Hadley (1997) have found a low-brightness arc outside the disk of M83 and explained it as the remnant of an accreted satellite. The global appearance of the H I disk could show some evidences of a past interaction, such as a large H I tidal feature that surrounds the optical disk of the galaxy (Park et al. 2001). At circumnuclear scales, it was found that the integrated Hα kinematical profile of the whole complex has a small secondary Gaussian component, redshifted with respect to the main one; and infall of material was claimed as a plausible explanation (Arsenault & Roy 1986). Moreover, it has been argued (Sofue & Wakamatsu 1994) that part of the central region of M83 is obscured by a polar dust lane, which in turn was related to a global warp in the H I disk. Coincidentally or not, the dust lane would end at the galactic equatorial plane in the region of the hidden mass concentration discussed here.

There are also a number of galaxies in which the optical nucleus is off centered with respect to the galaxy center, e.g., NGC 3227 (Mediavilla & Arribas 1993), M31 (Kormendy & Richstone 1995), NGC 1068 (Arribas et al. 1996), and NGC 5033 (Mediavilla et al. 2005). In many cases the off centering has been related to a galaxy merger, and minor mergers have been theoretically considered in the past as a source of gaseous nuclear fueling (Taniguchi & Wada 1996). It is expected in the above scenario that the nucleus of the cannibalized satellite is accreted to the central region of the galaxy, where theoretically it should generate a star formation trail (Saslaw & De Young 1972; Saslaw 1975) as it perturbs a gas rich environment and eventually produces a supermassive black hole binary. A statistical analysis of the previous photometric results (Harris et al. 2001) allows a quantitative approach to this proposition. We calculated the average age of the young massive clusters in 25° angular sectors of the 100° ringlet (within a radial range from 50 to 150 pc), and found a clear age gradient across the arc. This age gradient is more obvious when the age of the oldest clusters is considered; in the east extreme of the arc the oldest cluster is 25 Myr old, while in the northwest extreme, in the region of the intruder nucleus, the oldest cluster is only 5 Myr old. This age difference is beyond any statistical uncertainty; moreover, the appearance of the H II regions in Figure 1 shows clearly that the star-forming regions near the intruder nucleus are more compact and luminous, and therefore less evolved. Another striking characteristic of the giant arc of star formation is that the location of the youngest clusters and the Hα morphology indicate that the star formation has been radially propagated from the interior of the arc outward to its radial perimeter. As has been stated previously (Harris et al. 2001), it appears that the 5–7 Myr population has evacuated interstellar material from most of the active arc and that star formation is continuing along the radial edges of the region, where the gas density is probably still high. This phenomenon had no previous explanation, but would naturally fit in a scenario where star formation has propagated radially from the path of the intruder nucleus around the galactic center (see Figs.1 and 3). This picture is fully consistent with the dynamical crossing times of the galactic central regions, which have been estimated using the observed positions of the mass concentrations, the inferred path of the captured body in the circumnuclear region, and the rotation curve of M83 (Agüero & Díaz 2004) from optical, near-infrared, and radio observations. We consider that the orbit of the intruder mass is partially described by an ellipse with a semimajor axis not smaller than 120 pc (as seen in Fig. 1, and with the bulge center in one of the foci), a range of possible inclinations from the global one (20°–30°) to that inferred at the kinematical center (40°–60°), and the range of possible total masses enclosed in the radial range from 100 to 200 pc. This Keplerian approach gives a minimum dynamical crossing time of 3 Myr, and maximum of 12 Myr, with the most probable value around 5 Myr (semimajor axis 130 pc, inclination 45°, enclosed mass 2×10^8 $M_\odot$), which is fairly consistent with the age gradient depicted in Figure 1.

The observational evidences that would therefore support the proposed capture and star formation triggering picture are:

1. The hidden mass concentration is located at the younger end of the star-forming arc (Fig. 1).
2. The optical nucleus is out of the galactic geometry center and seems to have an associated stellar trail (see Figs. 1 and 3), possibly pointing toward the galactic center.
3. The continuum maps at radio wavelengths (Rogstad et al. 1974; Telesco 1988) and at 10 μm (Gallais et al. 1991; see our Fig. 3 for a superposition of the optical and mid-IR features) have a strong tidal appearance, with the largest emission at mid-infrared wavelengths located precisely at the position of the kinematically detected dark mass.
4. The mentioned possible off-plane dust lane related with global H I map (Sofue & Wakamatsu 1994) would end in the region of the hidden mass concentration.
5. The age of the oldest clusters in the starburst arc is about 25 Myr (Harris et al. 2001), similar to the dynamical crossing time of the central kiloparsec ($\sim$26 Myr).
6. The age difference between the youngest and the oldest ends of the arc (a few Myr) is similar to the dynamical crossing time at a hundred parsec scale in M83.

3.1. *Modeling*

In order to make a theoretical approach to the dynamical evolution of this kind of scenario, we simulate the encounter between the system components following the evolution of their stellar and gaseous contents. A set of numerical simulations were done using a TreeSPH code (Hernquist & Katz 1989). The circumnuclear galactic potential was represented by a fixed spherical Hernquist (1990) potential fitted to the most detailed rotation curve available for M83 (Agüero & Díaz 2004), with a total mass of 1.5×10^{11} $M_\odot$, scale length of 2.5 kpc, and cutoff radius of 40 kpc. It was centered at the bulge geometrical center, defined as the symmetry center of the outer *K*-band isophotes (see explanation in § 2). Nuclei models (optical nucleus and intruder nucleus) were

constructed following the general prescription for *N*-body galaxy realizations (Hernquist 1993), including gaseous and stellar disks plus a spherical component. Initial conditions for these models were based on the observed sizes, masses, and 2D radial velocity distributions. A total of 3000 particles were used for the mass distribution representing the optical nucleus, arranged in a disk component ($M_{\rm disk} = 0.9\times10^6\ M_\odot$; scale length $l = 4.2$ pc; vertical scale height $h = 0.4$ pc; $Q_{\rm Toomre} = 1.5$; $V_{\rm circ(peak)} = 25$ km s^{-1}) and a spherical component ($M_{\rm sphere} = 1.1\times10^6\ M_\odot$; core radius $r = 2.1$ pc; cutoff radius $r_{\rm cutoff} = 44$ pc). For the intruder nucleus we used 17,000 particles arranged in a disk component ($M_{\rm disk} = 8.8\times10^6\ M_\odot$; $l = 6.8$ pc; $h = 0.68$ pc; $Q_{\rm Toomre} = 1.5$; $V_{\rm circ(peak)} = 50$ km s^{-1}) plus a spherical component ($M_{\rm sphere} = 7.2\times10^6\ M_\odot$; $r = 3.4$ pc; cutoff radius $r_{\rm cutoff} = 68$ pc). Considering the observed molecular gas distribution (Lundgren et al. 2004), a fraction of 10% of the optical nucleus mass and 50% of the intruder dark mass were assigned to gaseous massive (SPH) particles.

As Figure 2 shows, Paβ spider-like diagrams, characteristic of a rotating disk, are observed around the kinematical center and hidden nucleus. Although they only indicate the gas behavior, the presence of a stellar disk cannot be ruled out, mainly around the kinematical center. This leads us to consider models composed of spheroids and disks in our simulations. Genzel et al. (2001) found that both nuclei of the major merger Arp 220 retain rotating gas disks; therefore, the presence of the disk in the intruder nucleus is physically possible. The real nature of the mass distribution would be determined when the NIR stellar velocity dispersion maps (currently under elaboration) become available. As a first approach to the problem, we model the intruder's orbit and the main galaxy disk coplanar, for the sake of simplicity and considering the strong star-forming effect on the main galaxy disk. Indeed, it has been shown in numerical simulations (Walker et al. 1996) and in the properties of double nuclei in spiral galaxies (Gimeno et al. 2004) that most of the accreted satellites would be moving in the disk of the main galaxy when they reach the circumnuclear region.

Figure 4 shows the evolution of the encounter in terms of the separation between the optical (original?) galaxy nucleus and the mass barycenter of the captured galaxy; the initial path was approached with a long parabolic orbit with a perigalactic distance $q = 1$ kpc. The models show that the main galaxy nucleus and the bulk of the intruder mass would form a single massive core in 50–70 Myr, considering the range of uncertainty in the orbit inclination. Note that this is, in fact, an upper limit, since in the present simulation the central potential of M83 is modeled by a rigid potential, and the dynamical friction between it and the optical and intruder nuclei is not considered. In fully self-consistent simulations under elaboration, the merging time may be considerably shorter. The massive core of a few $10^7\ M_\odot$ would finally settle as the new nucleus of M83 in less than 100 Myr, implying a net growth of the central galactic mass. Furthermore, the whole star formation and nuclei merging event would last less than a global galactic revolution (about 150 Myr at the average radius of 5 kpc). Mergers between spiral galaxies and their satellites are of broad interest because they can have a profound influence on the structure of disks in spiral galaxies through secular processes (Hernquist 1991; Combes 2001) that do not destroy the galaxy, unlike those events involving more massive companions (whose remnants are more akin to elliptical galaxies rather than any kind of spiral galaxy). Owing to the complexity of the merger process, quantitative predictions of the effects of merging are very difficult without appealing to numerical simulations applied to the study of individual events, which in turn can be used to constrain the models of spiral galaxy secular evolution. The massive core

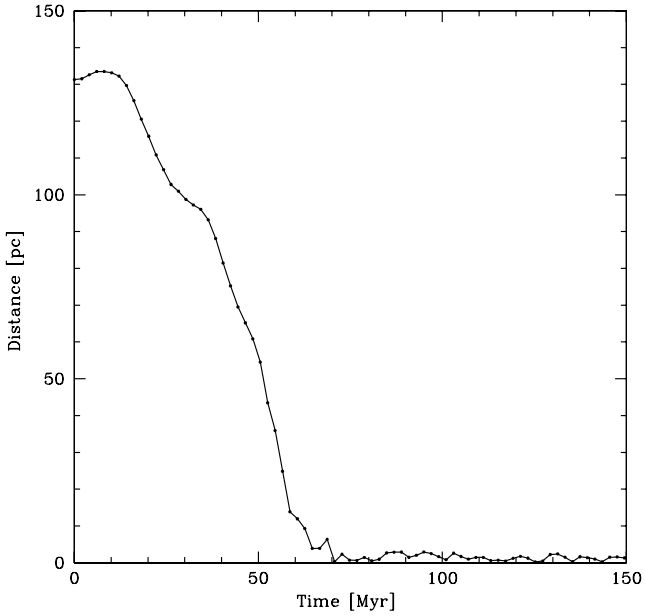

FIG. 4.—Evolution of the encounter in terms of the separation between the optical galaxy nucleus and the mass barycenter of the captured body. Time is shown with respect to the present configuration, and the range of uncertainty arises in the unknown orbit inclination. It can be seen that the optical original nucleus of M83 and most of the intruder mass would probably form a single massive core in 50–70 Myr. This massive core of a few $10^7 M_\odot$ would finally constitute the new nucleus of M83, implying a net growth of the central galactic mass.

of a few $10^7\ M_\odot$ that would finally settle as the new nucleus of M83 would represent about $10^{-3}\ M_{\rm acc}$, the mass that would be accreted during a Hubble time by a spiral galaxy such as our own (Hernquist 1991) or like M83, which would also be dynamically dominated by a massive halo (Agüero & Díaz 2004).

Whatever the origin of the interloper mass, its presence and star-forming trail are consistent with the suggestion that minor mergers and bar fueling are the main sources of bulge growth in spiral galaxies (Combes 2001), which in turn could explain the correlation between supermassive black hole mass and galactic bulge mass (e.g., Ferrarese & Merrit 2000; Tremaine et al. 2002; $M_{\rm SMBH} \sim 10^{-3} M_{\rm bulge}$). This correlation can be extrapolated to the Sbc morphological type of M83 and is consistent with the observations presented here: the presence of a quasar remnant ($M_{\rm SMBH} \sim 10^8\ M_\odot$) can be discarded in this spiral galaxy from our kinematic data. Notwithstanding, we might be in the presence of a circumnuclear disk caught in the last stages of the evolution toward a collapsed object with nonstellar activity. In this scenario the fate of M83 could be to evolve to an earlier type galaxy, eventually harboring an active nucleus, as might be expected from the statistical excess of active nuclei in Sa galaxies (Ho et al. 1997), which also ties bulge formation and evolution to massive black hole formation and evolution.

4. FINAL REMARKS

Summarizing, several pieces of observational evidence support the proposed capture and star formation triggering picture: (1) the hidden mass concentration, detected by 3D near-infrared spectroscopy, is precisely located at the younger end of the star forming arc; (2) the optical nucleus is out of the galactic geometry center and seems to have a stellar trail possibly pointing toward the geometric center; (3) the continuum maps at radio wavelengths and at 10 μm have a strong tidal appearance, with the largest emission at mid-infrared wavelengths located precisely

at the position of the kinematically detected dark mass; (4) a possible off-plane dust lane related to global H I map would end in the region of the hidden mass concentration; (5) the age of the oldest clusters in the starburst arc would be about 25 Myr, similar to the dynamical crossing time of the central kiloparsec (∼26 Myr); and (6) the age difference between the youngest and the oldest ends of the arc (a few Myr) would be similar to the dynamical crossing time at a hundred parsec scale in M83. Therefore, the hidden mass location and the inferred average cluster ages and the dynamical times clearly indicate that the interloper has left behind a spur of violent star formation in M83, in a transient event lasting less than one orbital revolution.

The origin of the interloper could be bar-funneled material or a cannibalized satellite, and the fate of most of the involved masses could be a black hole merging or giant stellar cluster. Whatever the nature and fate of this complex system, we surely (and luckily) are witnessing a short event that yields a net growth of the galactic core in this grand-design spiral galaxy, and the phenomena reported here should help to make a leap forward in our understanding of the evolutionary picture of the final stages in a galactic minor merger or a bar-funneled massive cloud. We remark that the reported ages and timescales imply that the observed phenomenon is extremely short in galactic timescales (probability of occurrence less than 1% in a given galaxy), and that its detection may be unique among the nearby galaxies. The next step in our study is the execution of higher resolution numerical studies, together with spectroscopic and imaging observations in the mid-infrared range, focused on the (dark) largest dynamical center, which so far appears to be bright at these wavelengths.

R. D. thanks the support of the Instituto de Astrofisica de Canarias (Spain) and the hospitality of its researchers. H. D. acknowledges support from CNPq (Brazil) and Megalit/Millennium grants. E. M. thanks the support of the Euro3D RTN. We wish to thank the Instrumentation Group at the Institute of Astronomy, Cambridge, for providing CIRPASS and supporting the observations at the telescope. The Raymond and Beverly Sackler Foundation and PPARC were responsible for the funding of CIRPASS. Finally, we acknowledge the Gemini Observatory for the allocation of telescope time, allowing CIRPASS to be used as a visitor instrument. The Gemini Observatory is operated by the Association of Universities for Research in Astronomy, Inc., under a cooperative agreement with the NSF on behalf of the Gemini partnership: NSF (US), PPARC (UK), NRC (Canada), ARC (Australia), CONICET (Argentina), CNPq (Brazil), and CONICYT (Chile). The NASA/ESA *Hubble Space Telescope* is operated by AURA under NASA contract NAS 5-26555. This work also was partially supported by the CONICET grant PIP 5697.

REFERENCES

Agüero, M., & Díaz, R. J. 2004, Bull. Assoc. Argentina Astron., 47, 360
Arribas, S., Mediavilla, E., & Garcia-Lorenzo, B. 1996, ApJ, 463, 509
Arsenault, R., & Roy, J.-R. 1986, AJ, 92, 567
Athanassoula, E. 1992, MNRAS, 259, 345
Binney, J., & Tremaine, S. 1987, Galactic Dynamics (Princeton: Princeton Univ. Press)
Combes, F. 2001, in The Starburst-AGN Connection, ed. I. Aretxaga, D. Kunth, & R. Mujica (Singapore: World Scientific), 223
de Vaucouleurs, G., de Vaucouleurs, A., Corwin, H., Buta, R., Paturel, G., & Fouque, P. 1991, Third Reference Catalogue of Bright Galaxies (New York: Springer) (RC3)
Díaz, R. J., Carranza, G., Dottori, H., & Goldes, G. 1999, ApJ, 512, 623
Elmegreen, D., Chromey, F., & Warren, A. 1998, AJ, 116, 2834
Ferrarese, L., & Merritt, D. A. 2000, ApJ, 539, L9
Gallais, P., Rouan, D., Lacombe, F., Tiphene, D., & Vauglin, I. 1991, A&A, 243, 309
Genzel, R., Tacconi, L., Rigopoulou, D., Lutz, D., & Tecza, M. 2001, ApJ, 563, 527
Gimeno, G., Díaz, R. J., & Carranza, G. 2004, AJ, 128, 62
Handa, T., Nakai, N., Sofue, Y., Hayashi, M., & Fujimoto, M. 1990, PASJ, 42, 1
Harris, J., Calzetti, D., Gallagher, J., Conselice, C., & Smith, D. 2001, AJ, 122, 3046
Heller, C., & Shlosman, I. 1994, ApJ, 424, 84
Hernquist, L. 1990, ApJ, 356, 359
———. 1991, in Warped Disks and Inclined Rings around Galaxies, ed. S. Casertano et al. (Cambridge: Cambridge Univ. Press), 96
———. 1993, ApJS, 86, 389
Hernquist, L., & Katz, N. 1989, ApJS, 70, 419
Ho, L., Filippenko, A., & Sargent, W. 1997, ApJ, 487, 568
Kenney, J., & Lord, S. 1991, ApJ, 381, 118
Kormendy, J., & Richstone, D. 1995, ARA&A, 33, 581
Lundgren, A., Wiklind, T., Olofsson, H., & Rydbeck, G. 2004, A&A, 413, 505
Maciejewski, W., & Sparke, L. 2000, MNRAS, 313, 745
Malin, D., & Hadley, B. 1997, Publ. Astron. Soc. Australia, 14, 52
Mast, D., Díaz, R. J., & Agüero, M. 2006, AJ, 131, 1394
Mast, D., Díaz, R. J., Agüero, M. P., Weidmann, W., Carranza, G., & Gimeno, G. 2002, Bull. Assoc. Argentina Astron., 45, 74
Mediavilla, E., & Arribas, S. 1993, Nature, 365, 420
Mediavilla, E., Guijarro, A., Castillo-Morales, A., Jiménez-Vicente, J., Florido, E., Arribas, S., García-Lorenzo, B., & Battaner, E. 2005, A&A, 433, 79
Park, O., Kalnajs, A., Freeman, K., Koribalski, B., Staveley-Smith, L., & Malin, D. 2001, in ASP Conf. Ser. 230, Galaxy Disks and Disk Galaxies, ed. J. G. Funes & E. M. Corsini (San Francisco: ASP), 109
Parry, I., et al. 2000, Proc. SPIE, 4008, 1193
Petitpas, G., & Wilson, C. 1998, ApJ, 503, 219
Pinner, B. G., Stone, J. M., & Teuben, P. J. 1995, ApJ, 449, 508
Rogstad, D., Lockart, I., & Wright, M. 1974, ApJ, 193, 309
Sakamoto, K., Matsushita, S., Peck, A., Wiedner, M., & Iono, D. 2004, ApJ 616, L59
Saslaw, W. C. 1975, in IAU Symp. 69, Dynamics of Stellar Systems, ed. A. Hayli (Dordrecht: Reidel), 379
Saslaw, W. C., & De Young, D. 1972, ApJ, 11, L87
Sérsic, J. L., & Pastoriza, M. 1965, PASP, 77, 287
Sofue, Y., & Wakamatsu, K. 1994, AJ, 107, 1018
Taniguchi, Y., & Wada, K. 1996, ApJ, 469, 581
Telesco, C. M. 1988, ARA&A, 26, 343
Thatte, N., Tecza, M., & Genzel, R. 2000, A&A, 364, L47
Tremaine, S., et al. 2002, ApJ, 574, 740
Walker, I., Mihos, J., & Hernquist, L. 1996, ApJ, 460, 121